JOURNAL GEOLOGICAL SOCIETY OF INDIA
Vol.95, February 2020, pp.197-204

Integrated Geological and Geophysical Approach to Reservoir Modeling: Case Study of Jambi Sub-basin, Sumatra, Indonesia

Abdul Haris
Geology Study Program, Faculty of Mathematics and Natural Sciences, Universitas Indonesia, Depok, 16424, Indonesia
E-mail: *abdulharis@sci.ui.ac.id*

ABSTRACT

Integrated geological and geophysical investigations were successfully performed for reservoir modeling in an oil field in the Jambi Province sub-basin, Sumatra, Indonesia. The objective of this study is to characterize the oil reservoir in terms of its petrophysical properties using a facies model that is based on an integrated geological and geophysical approach. The reservoir target of this study is located in the Air Benakat Formation, which is identified with a thickness of 3 to 20 m and is deposited in a depth range of 1300–1500 m. The reservoir modeling of Air Benakat Formation is carried out to open a new discovery for this field, since the comprehensive reservoir modeling has not been intensively performed. Structurally, the reservoir is segmented into three compartments by four main faults, and stratigraphic investigations revealed three prospect layers. In the present framework of the depositional environment, assessments of well log data included formation evaluations, well log data correlations and sequence stratigraphy, were performed to produce high-resolution features of vertical and lateral distributions. In addition, seismic data were interpreted to guide the structural model, and to effectively construct a three-dimensional (3D) geological framework of reservoir properties. The modeled reservoir shows that the reservoir is primarily considered a transition zone to a shallow marine deposit, which is specifically located in a submarine fan channel with a plain/moderately steep angle of its sedimentation base. Depositional environments are generally characterized by the potential paleocurrent direction within the channel axis from NE to SW, with respective agreement from larger scale porosity and net/gross models.

INTRODUCTION

For more than a century the south Sumatra basin has been actively explored. This basin contains around 23% of the total conventional hydrocarbon reserves in Indonesia (Rudd, et al., 2013). However, in the last few years there has been no discovery of new reserves which make hydrocarbon production in this basin continue to decline from year to year. This situation is occurred in this study area whose production is continuously decreasing, thereby the effort need to be performed to optimize hydrocarbon resources that have not yet been produced. In order to realize the efforts, static reservoir modeling is needed to characterize and map the reservoir distribution. Moreover, the hydrocarbon reserve, which can be used for reservoir simulation, can be estimated.

The study area is in the Jambi sub-basin of the south Sumatra Basin, and is located in Muaro Jambi district, Jambi province, about 10 km southeast of Jambi city (Fig. 1). This basin is categorized as a back-arc basin and is confined by Tigapuluh mountains and separated by the Duabelas mountains to the Central Sumatra basin (Lutz et al., 2011). This basin is also constrained by the Sempilang hills in the southeast, the Lupak hills in the northeast, and the Malaka Strait in the east (Haris et al., 2017).

The Jambi sub-basin was formed in the late Paleozoic to the mid-Mesozoic era and is surrounded by the Barisan Mountains, the Tigapuluh mountains, the Duabelas mountains and other mountains in the south Sumatra region. According to historical tectonic movements, this basin was formed in four episodes (De Coster 1974), including the mid-Mesozoic orogenesis, the late Carboneous–early Tertiary tectonic, the tectonic quiescence, and the Pliocene–Pleistocene orogenesis. The first episode was started at the mid-Mesozoic orogenesis, where sediments were deposited and then heated to form metamorphic rocks in the mid-Mesozoic. During the late Carboneous–early Tertiary tectonics, the basin was formed through a specialized regional extension that formed graben and fault blocks running in a north to south or northwest to southeast directions, with some running west to east. The formation was then continued to tectonic quiescence in the early Tertiary to Miocene era. During this episode, subsidence of the basin platform was the major event and led to the formation of Tertiary sediments. These forming episodes were concluded by the Pliocene–Pleistocene orogenesis, which led to the formation of a massive fold and faults running to the northwest (Sarjono, 1989; McClay and Bonora, 2001).

The petroleum system of the Jambi sub-basin is characterized by source rocks of black shale in Lemat Formation, and these are known as members of Benakat clay, lignite, and shale of the Talang Akar Formation and shale of the Telisa Formation (Kasim and Armstrong, 2015; Maulana and Haris, 2018). Typical reservoirs in this basin are classified as sandstone and limestone (Argakoesoemah and Kamal, 2004) and sandstone reservoirs are dominant in the upper Lemat formation and Talang Akar Formation, and in the lower and middle parts of the Palembang Formation, whereas limestone reservoirs are

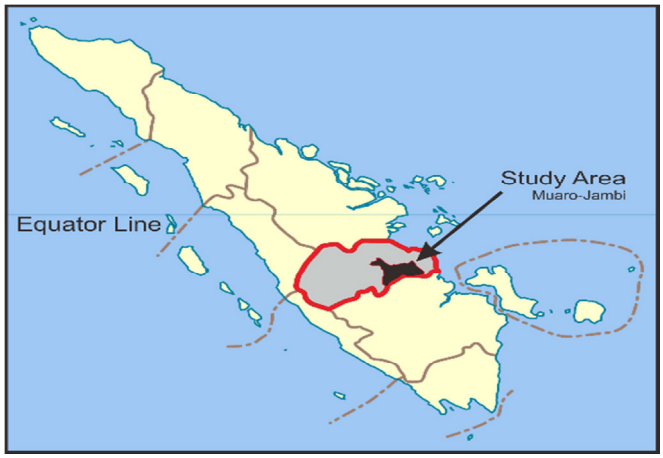

Fig.1. The map of study area in the Jambi sub-basin, Sumatra, Indonesia, which is indicated by the black shadow in the red polygon.

0016-7622/2020-95-2-197/$ 1.00 © GEOL. SOC. INDIA | DOI: 10.1007/s12594-020-1410-7

present in the Telisa Formation, which is well known as Baturaja Carbonates. The seal rock in this basin is commonly shale, which is thick in Telisa, lower Palembang, and middle Palembang formations (Bishop, 2001). This seal rock comprises laterally variable facies and/or faults that are stratigraphical and structural. In addition, hydrocarbon migrations in this field could be lateral, although secondary migration is the main mode of transport that leads to accumulation of hydrocarbons in the reservoir (van Bemmelen, 1949; De Coster, 1974).

Many studies have been conducted on several fields in this basin, such as sequence stratigraphic analysis, which refer to well log and outcrop data (Melati and Apriadi, 2018), depositional environment analysis using attribute spectral decomposition (Rizaldi and Fauzi, 2015), and facies modeling (Ariani, et al., 2010). On the other hand, most of the previous studies were only carried out in the eastern part of the basin rather than the western part of the basin. Thereby this paper presents the reservoir property modeling of the field in the western part of the basin, which were constrained by facies model. The challenges of this field are not only structural uncertainty but also facies and petrophysics problems (Susanto, 2009).

Therefore, an integrated geological and geophysical approach instead of doing reservoir maping (Haris et al., 2017; Maulana and Haris, 2018) for determining the petrophysical properties of the Air Benakat Formation of Jambi sub-basin, Sumatra, Indonesia using a structural and stratigraphic seismic and facies reservoir model is presented. The integrated geological and geophysical approach is expected to obtain comprehensive analysis since the cost of the advanced development phase up to 20-50% of an oil and gas project (Rui et al., 2018).

Reservoir modeling was performed by incorporating core and well log analyses into geological and facies models. These studies were based on data from 15 well logs and from 3D seismic cube data covering an area of 30 km^2. The reservoir model offers useful information that can be used to characterize the oil reservoir.

GEOLOGICAL AND GEOPHYSICAL APPROACH

Geological investigations were performed by assessing sediment cores, well log data, and well log correlations to obtain vertical and lateral distributions of the depositional environmental pattern in a framework of the reservoir architecture (Ito et al., 2017; Mode et al., 2017). This geological approach must be supported by geophysical investigations to provide a structural and stratigraphic model that effectively reconstructs the 3D geological framework of reservoir properties (dos Anjos and Zucchi, 2001; Corbell and Wellmann, 2015). In general, the sequence of geological and geophysical approaches is performed using petrophysical analysis, well log correlations, and sequence stratigraphic analyses (Melati and Apriadi, 2018). The detailed workflow for reservoir modeling, which is based on the geological and geophysical approaches, is presented in Fig.2.

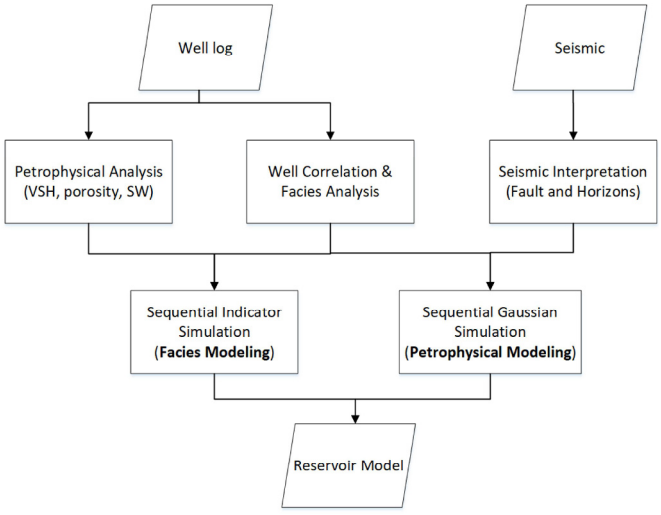

Fig. 2. The detailed workflow for reservoir modeling, which is based on the geological (well log data) and geophysical (seismic data) approaches.

Petrophysical Data

Petrophysical analyses are crucial to reservoir modeling because the physical parameters of rocks provide a reference for delineating reservoir and non-reservoir distributions (Bornard et al., 2005; Elsayed et al., 1993). Seven well log data were selected for petrophysical analyses of porosity, shale volume, and water saturation, and were derived in formation evaluations. The stratigraphic model was then generated by identifying the continuation of lateral distributions of depositional environmental changes, which were based on the well correlation in a framework of sequence stratigraphy. Further, the well correlations were performed chronostratigraphically rather than using lithotype correlations (Mitchum et al., 1977). Well, correlations were then used to identify depths and thicknesses of the reservoirs at each well location.

In addition, petrophysical analyses were performed to assess petrophysical data, which were required for the building of the 3D reservoir model. The main properties presented in this reservoir model are shale volume, porosity, water saturation, and cut-off parameters.

Shale Volume

Shale volume was calculated based on equation 1, which refer to a cut-off selection of baseline gamma ray (GR) for each stratigraphic formation (Das and Chatterjee, 2018). The calculated shale volume was then used to define facies into classes of sandstone and shale with reference to the X-13 well, the GR for clean sand showed an American Petroleum Institute (API) of 36, and for clean shale the maximum GR was 116 API. Facies depth intervals of sandstones and shales were then defined for the whole depth of well log data. Previous studies identified sandstone with a GR of less than 50 API and shale with GR of greater than 90 API. Panel 3 of Fig. 3 shows the GR log for identifying clean sand and clean shale.

$$V_{sh} = \frac{(GR - GR_{min})}{(GR_{max} - GR_{min})} \quad (1)$$

where GR = gamma ray log, GR_{min} = minimum gamma ray as a clean sand, GR_{max} = maximum gamma ray as shale-based line, and V_{sh} = shale volume.

In reservoir modeling, the shale volume parameter is then converted to a net-to-gross ratio, which is a parameter that shows the thickness of the clean sand layer divided by the total thickness of the reservoir. Net-to-gross ratio of one means that all reservoir intervals are clean sand. The parameter of net-to-gross ratio is required to predict the hydrocarbon pore feet, which is input to overall reservoir original hydrocarbon in place calculation.

Porosity

Pore spaces of reservoir layers are represented by neutron, density, and by a combination of both logs. The modeled porosity from density log was calculated using equation 2, while the neutron-density porosity was calculated using equation 3. Whereas all porosity models were constructed to determine the porosity of the target reservoir, the selected model is the best porosity model, as indicated by good agreement with the porosity of core samples (Fig. 3). This step was becoming important before the calculated porosity is spatially distributed by seismic data and geostatistical approach (Das and Chatterjee, 2016; Kumar et al., 2018). Therefore, the combined neutron density porosity

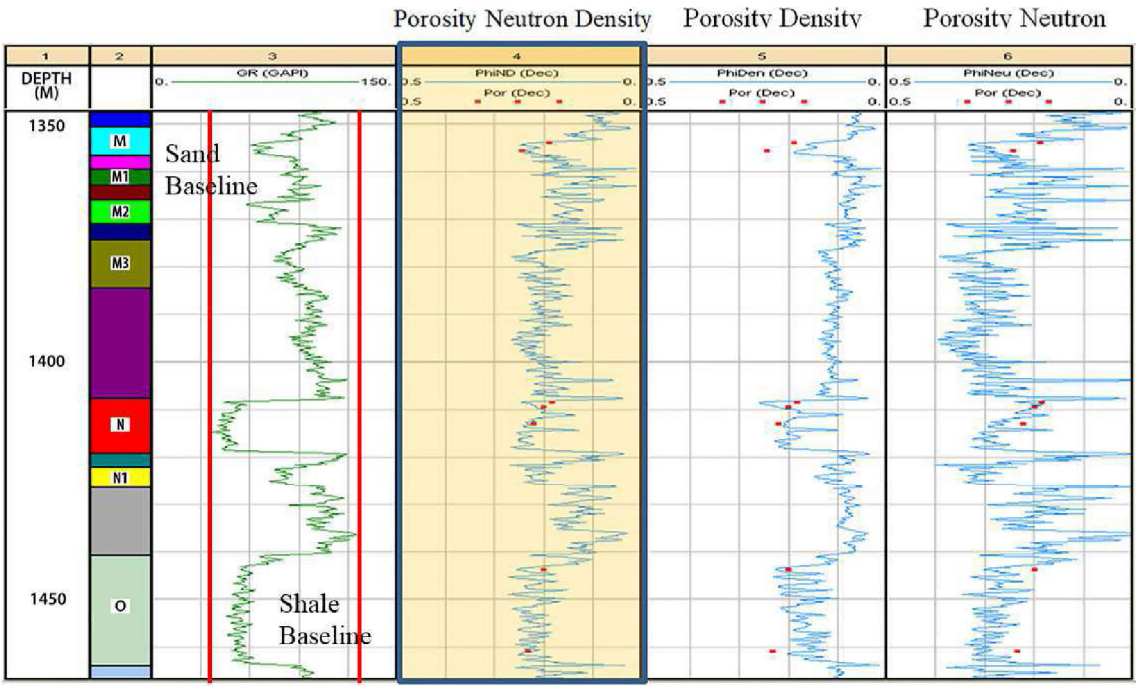

Fig. 3. The comparison of porosity models (solid blue line) and porosity of core samples (red dot) for X-13 well. Panel 4 shows the best fit between porosity models of combined neutron density and porosity of core samples.

model was selected as the porosity model for this study area. Panel 4 of Fig. 3 shows the best fit between porosity models of combined neutron density and porosity of core samples. The two other panels (panels 5 and 6) show slight deviations compared with the porosity of core samples. Furthermore, the selected porosity model was then applied to all wells that have no porosity data from rock samples. However, for wells that do not have a porosity log, we used a porosity calculation method that is based on the control of shale contents (Moradi et al., 2016).

$$\phi_{density} = \frac{(\rho_{log} - \rho_{matrix})}{(\rho_{fluid} - \rho_{matrix})} \quad (2)$$

$$\phi_{ND} = \frac{(\rho_{neutron} - \rho_{density})}{2} \quad (3)$$

where, ρ_{log} = density log, ρ_{matrix} = matrix density (Quartz = 2.65 gr/cc), ρ_{fluid} = fluid density (water = 1 gr/cc), $\phi_{density}$ = porosity density, $\rho_{neutron}$ = porosity neutron, ϕ_{ND} = porosity neutron-density.

Water Saturation

Water portions of pore space volumes are a critical determinate of the reservoir model, and calculations of water saturation need to be conducted carefully. Calculated water saturation values in the present study area varied between zones even though they were calculated using the same method. Thus, water saturation was calculated using the Indonesian saturation model as shown in equation 4 (Poupon and Leveaux, 1971; Shedid and Saad, 2017), which is considered representative of a reservoir with a characteristic sand-shale interlayer.

$$W = \left\{ \frac{\sqrt{\frac{1}{Rt}}}{\left(\frac{Vsh^{(1-0.5Vsh)}}{\sqrt{Rsh}}\right) + \sqrt{\frac{{\phi_e}^m}{a.Rw}}} \right\}^{(2/n)} \quad (4)$$

where Rt = formation resistivity, Vsh = shale volume, Rsh = resistivity of shale, ϕ_e = effective porosity, Rw = water resistivity, a = cementation constant, m = cementation exponent, n = saturation exponent, and SW = water saturation.

Formation resistivity is one of the main parameters required to determine hydrocarbon saturation. In these analyses, electric current flows through rock formations due to the conductivity of water in pores and clay molecules. In contrast, dry rocks and hydrocarbons are good insulators, except when minerals such as graphite and iron are present. Because no special core data analyses were available to determine Archie parameter values (a, m, and n), we used standard parameters that are generally used for sand reservoirs as follows: a = 0.62, m = 2.15, and n = 2 (Archie, 1950). We assumed that these values represent the reservoir of the study area.

Well Log Data Correlation

To delineate lateral stratigraphic distributions, well log correlations over key wells in the study area by reading GR logs was calculated so that correlations were based on continuous lithology. In general, the sand-shale profile is shown by a different depositional cycle, which is indicated by coarsening and fining upward. These cycles were previously associated with regressive and transgressive sequences (Catuneanu, 2006; Allen and Johnson, 2011). In addition, the well correlation was performed by defining the sequence stratigraphic framework with facies analyses in each well. Petrophysical analyses for each well were used to interpret lithofacies and their lateral distributions. The ensuing well correlation was based on the Air Benakat Formation, which is dominated by sandstones and claystone (M and N layer). This depositional sequence, which was bounded by top and bottom sequence boundaries, was reportedly recognized by a regressive and transgressive cycle (Ito et al., 2017). Finally, the sequence stratigraphic model was constructed using sequence boundaries that were identified at each well.

Seismic Interpretation

The unique characters of seismic reflections allow direct characterization of geological compositions. Seismic reflection, which is generated by the contrast of acoustic impedances between layers, indicates areas of stratigraphic conformity and nonconformity. Thus,

from seismic sections, we can identify a lithostratigraphy that reflects formations at certain depths, and patterns with geological structures. These seismic interpretations strongly influenced our reservoir modeling, and we used all available 3D seismic data. Prior to seismic interpretation, seismic data conditioning was performed for noise suppression, quality improvement, and seismic well tie (Das et al., 2017).

The seismic well tie was used to correlate seismic data with geological information from well log data. Accordingly, the sequence boundary that was defined in the well log data can be traced to its lateral distribution by observing the seismic data. In addition, the seismic interpretation was performed to define the horizon and fault structure.

RESERVOIR MODELING

The present reservoir model is focused on lateral distributions of petrophysical properties of the target layer and is intended as a preliminary for construction of a proper model that better approximates the real sub-surface geological conditions. After analyzing petrophysical properties and constructing a geometrical framework, we applied the sequential Gaussian simulation (SGS) geostatistical algorithm (Pyrcz, 2014). Stochastic modeling of continuous variables was performed using the SGS algorithm to integrate seismic data, which guided the construction of a geometric framework of the reservoir, and well log data that confirmed petrophysical properties through lateral distributions of porosity, water saturation, and net/gross. This algorithm is known as a kriging technique and uses spatial correlations and sequential conditional simulations based on a variogram. Due to limitations of well log data, it is not always easy to generate variograms. Thus, we used 3D seismic data to define the geometrical framework of reservoir properties in a lateral distribution.

Prior to laterally distributing petrophysical properties of the reservoir, we generated a facies model that was directly derived from integrated petrophysical and geophysical analyses. Facies modeling was based on geological approximations from lithological correlations of well log data that indicate lateral distributions and sequence stratigraphy analyses, which were compared with eustacy and petrography analyses to interpret environmental sedimentation (Hoyanagi et al., 2000). In this work, facies were determined in sand and shale that developed in the N layer. To laterally distribute these facies, we used the sequential indicator simulation (SIS) algorithm, which is constrained by the root mean square of seismic amplitude and regional facies. The previous research papers confirmed that the facies and depositional environment control the reservoir properties quality such as porosity and net-to-gross ratio (Al-Eidan et al., 2001; Sprague et al., 2005). Therefor, the property modelling was performed by referring the facies modelling.

RESULTS AND DISCUSSION

Figure 4 generally illustrates the petrophysical analyses of well log data, which includes geological marker, gamma ray, porosity (N-PHI & Rho-B), resistivity, salinity, water saturation, perforation test, porosity and lithology from left to right panel respectively. The water saturation calculation in panel 7 of Fig. 4 was performed in a two-depth range with low water saturation. The first depth range was 1407–1418 m and the second was 1440–1460 m. These depth ranges reflected the presence of a potential layer of the reservoir, and this layer was confirmed by the lithology log shown in panel 10. Panel 8 of Fig. 4

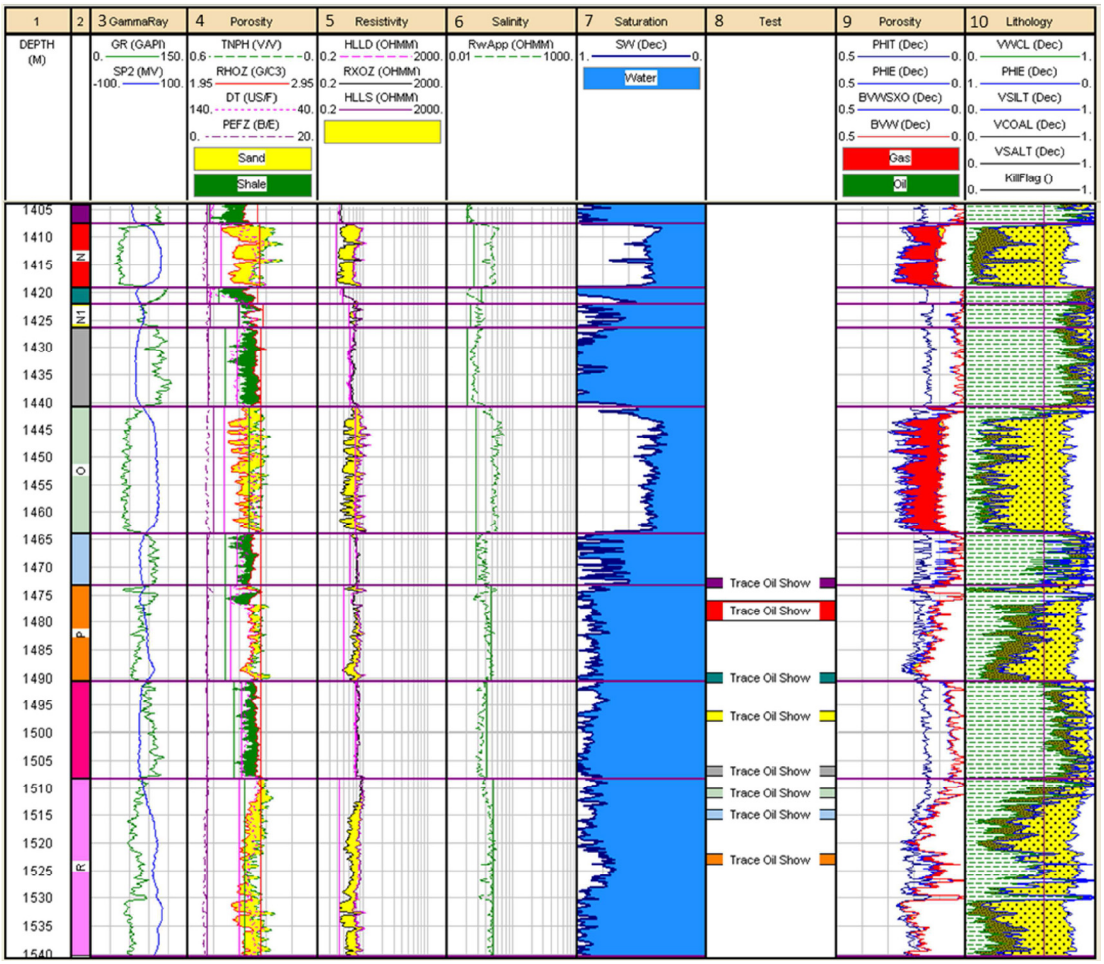

Fig. 4. The petrophysical analysis of well log data, including porosity (panel 4), water saturation (panel 7), and lithology (panel 10). The panel 8 show results of perforation, which is used as a quality control for log interpretations.

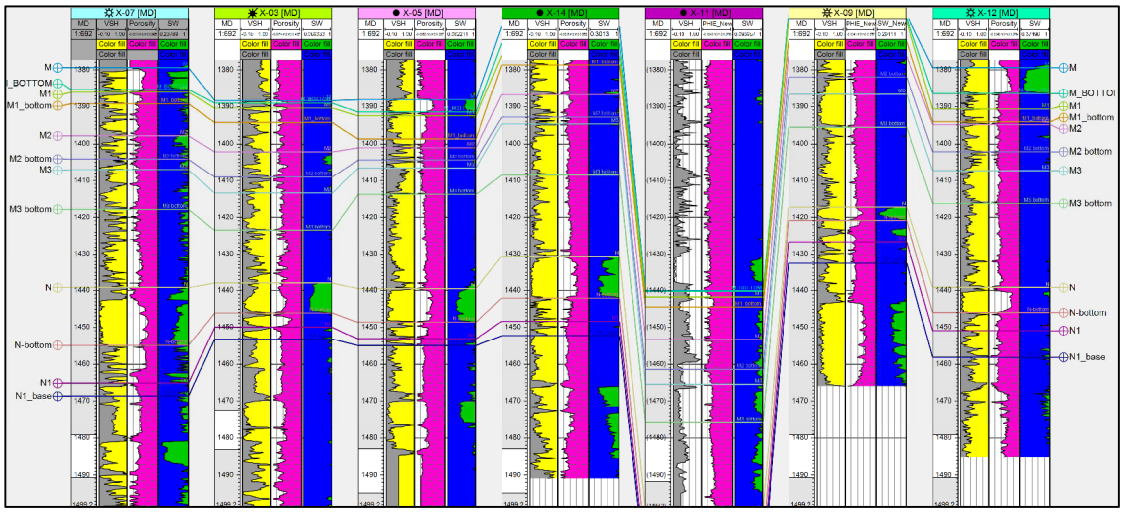

Fig. 5. The summary of the petrophysical analysis that contains shale volume, porosity and water saturation for the seven wells (X-07, X-03, X-05, X-14, X-11, X-09, and X-12).

shows the perforation test for a certain depth and was used to verify petrophysical analyses.

The summary of the petrophysical analysis that contains shale volume, porosity and water saturation of the seven wells are shown in Fig. 5. The classified layers were correlated among the seven wells, which included six layers (M, M1, M2, M3, N and N1). Each of the layer was represented by the top and bottom geological marker. Refer to the petrophysical analysis, it is found that layer N is classified to be one of the potential layers. The layer N is then selected as the main target for reservoir modeling. The detailed petrophysical parameter for layer N, which covered the seven wells is presented in Table 1.

Table 1. The detailed petrophysical parameter for layer N for the seven wells.

No	Well Name	*Vsh*	Porosity	*SW*
1	X-07	0.089	0.198	0.630
2	X-03	0.119	0.169	0.591
3	X-05	0.082	0.190	0.471
4	X-14	0.089	0.194	0.406
5	X-11	0.098	0.186	0.423
6	X-09	0.063	0.165	0.968
7	X-12	0.064	0.247	0.869

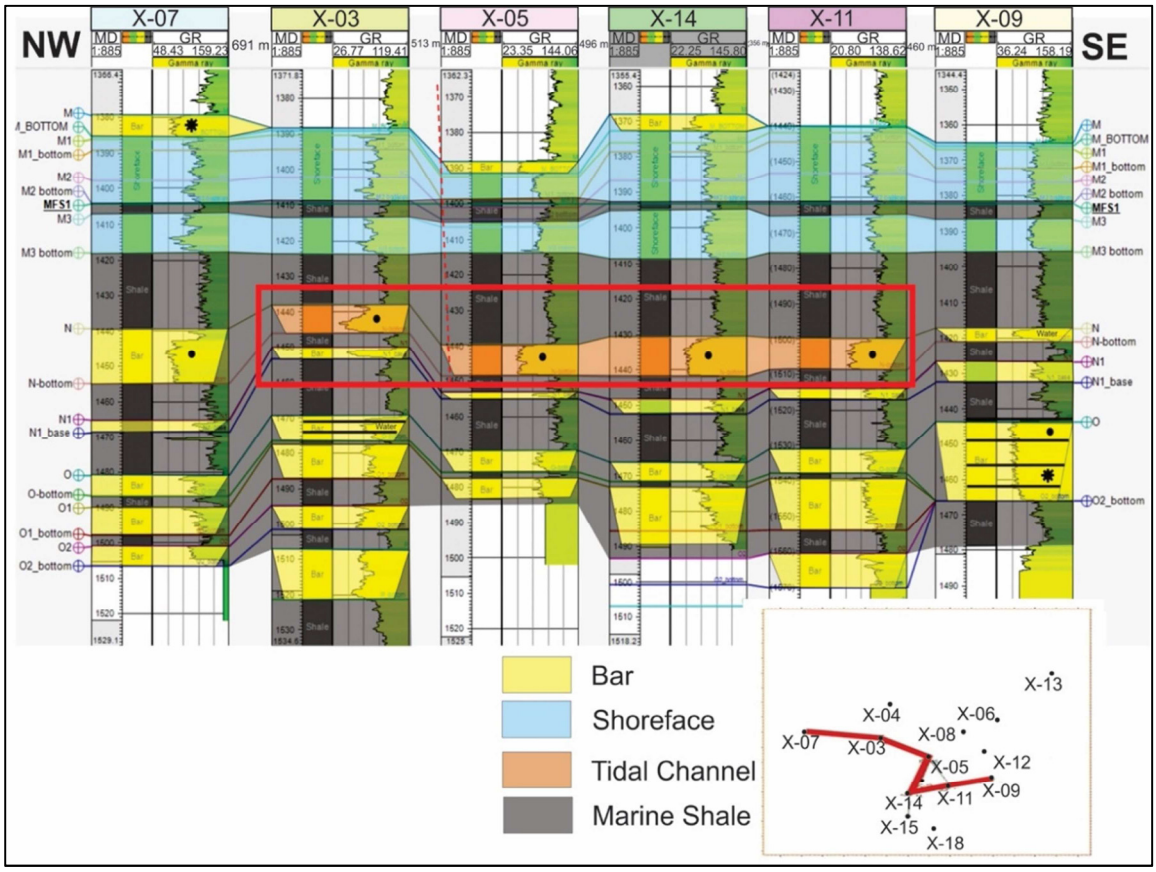

Fig. 6. The correlations of key well logs that illustrate depositional cycles in sand-shale profiles. The index map show the traverse path of well correlation (X-07, X-03, X-05, X-14, X11, and X-09).

There are two wells that showed less prospect, which were indicated by high water saturation; i.e., well X-09 and well X-12.

Figure 6 shows log correlations of the six wells that illustrate the lateral stratigraphic framework. These well correlations illustrated the depositional cycles found in sand-shale profiles for each well. Moreover, the multiple stacking channel deposit was identified in the Air Benakat formation. This channel was formed during rifting and has geometrical potential to be a reservoir. The red box in this figure highlights the sand continuity, which is interpreted as a meandering submarine fan channel. The isolated well on the northwestern part of the correlation was interpreted as a point bar channel fill in the meandering mechanism. However, characteristics of the tidal channel need to be evaluated because this channel may have large hydrocarbon contents and may thus influence the reserve calculation of the static model.

Based on well log correlations, four wells (X-03, X-05, X-14, and X-11) with NW-SE distribution indicated sand deposits in N layers, which are associated with the marine tidal channel. In particular, well X-03 showed that the tidal channel, which is a main concern for the reservoir model, occurs at a depth of 1400-1420 m and is formed in a solitary deposit. This solitary deposit is interpreted as an abandoned submarine fan lobe and is strongly influenced by the channel bar of this system. Wells X-05, X-11, and X-14 show significant tidal channel deposits that correlate with each body of the channel. We interpreted these correlate bodies as the main body for the reservoir model, with NW-SE width trending of the channel and NW-SW trending of the paleocurrent according to the basin configuration.

Horizon picking was performed by referring to the marker of the reservoir target, and the four picked horizons were identified in the seismic section, as illustrated in Fig. 7 Furthermore, this horizon was then used as a boundary to define the geometrical framework of the reservoir.

Structural features of the study area include a two-fault system trending NE-SW, and its tips are terminated by a normal fault inside the system. These features are associated with the latest tectonic phase, which was reactivated by the Pliocene-Pleistocene orogenesis and led to the formation of a massive fold and fault directed toward the NW (De Coster, 1974). According to this flexural analysis, we conclude that our main reservoir is cut by a single major strike-slip system, which is followed by a releasing bend movement in the extensional region (Harding et al., 1985). These structural features are shown in the index map of Fig. 7.

Figure 8 shows the modeled reservoir in terms of facies, porosity, water saturation, and net/gross properties. The facies model in Fig. 8(a) shows a meandering toward a braided type of channel that is classified as a tidal channel and likely developed under marine fan conditions and propagated a tidal sand deposit. This channel was interpreted as the main body for the reservoir model, with NW-SE width trending and NW-SW trending of the paleocurrent according to the basin configuration. The channel axis and channel bar are filled with a sandbar deposit, which has a similar predicted average porosity of around 0.15-0.2, as indicated by the porosity distribution in Fig. 8(b). This porosity distribution is guided by the facies model and provided good geological agreement. In addition, similar to the facies model, the porosity distribution tends in a NE-S direction.

Fig, 8(c) shows the water saturation distribution. Average water saturation along the channel axis was predicted to range from 0.2 to 0.3 and was slightly greater within the sandbar, where it ranged from 0.7 to 0.8. According to the net/gross distribution shown in Fig. 8(d), the N layer has a greater value at the channel axis, ranging from 0.6 to 0.8, than the sandbar, which ranges from 0.3 to 0.4.

In general, the reservoir has been properly modeled, and the geological aspect that controlled the major reservoir is well represented as a gross depositional environment. The reservoir is primarily considered a transition zone to a shallow marine deposit, which is specifically located in a submarine fan channel with a plain/moderately steep angle of its sedimentation base.

The fence diagram analysis in Fig. 9 shows the orientation of the channel, and the geometry also can be identified by meandering from

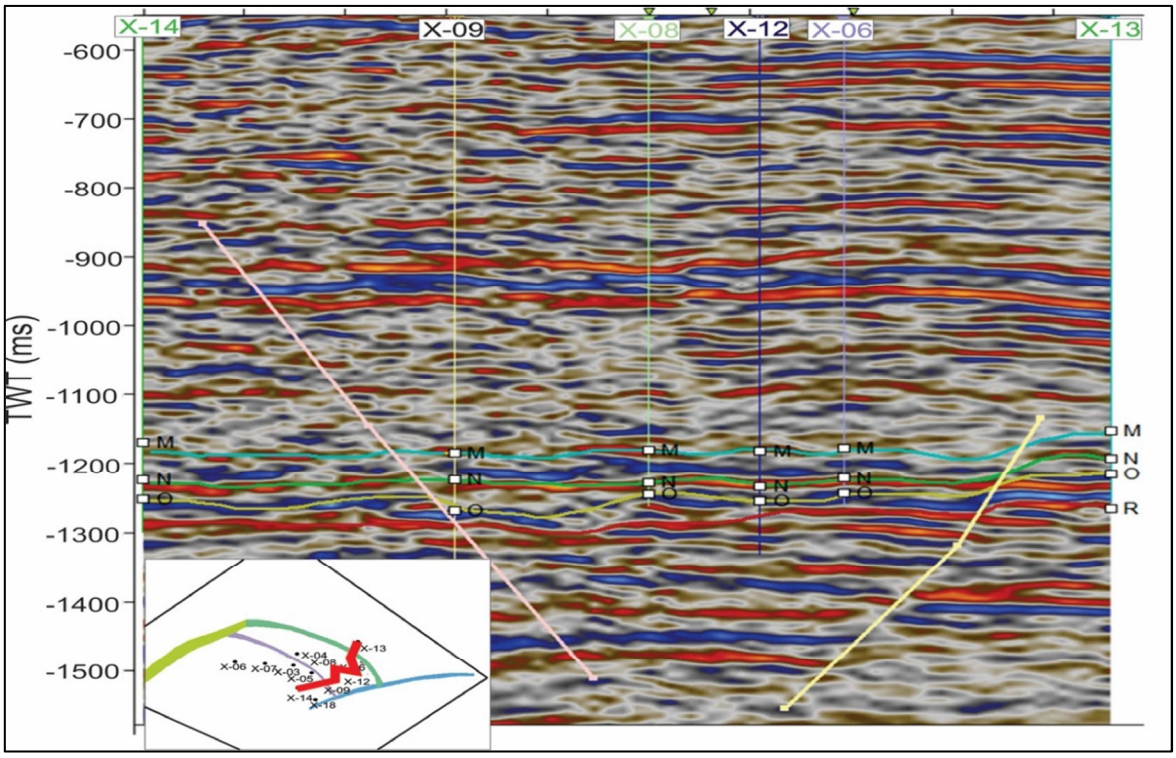

Fig. 7. The seismic interpretation for identifying the horizon and fault in a traverse path crossing among key wells.

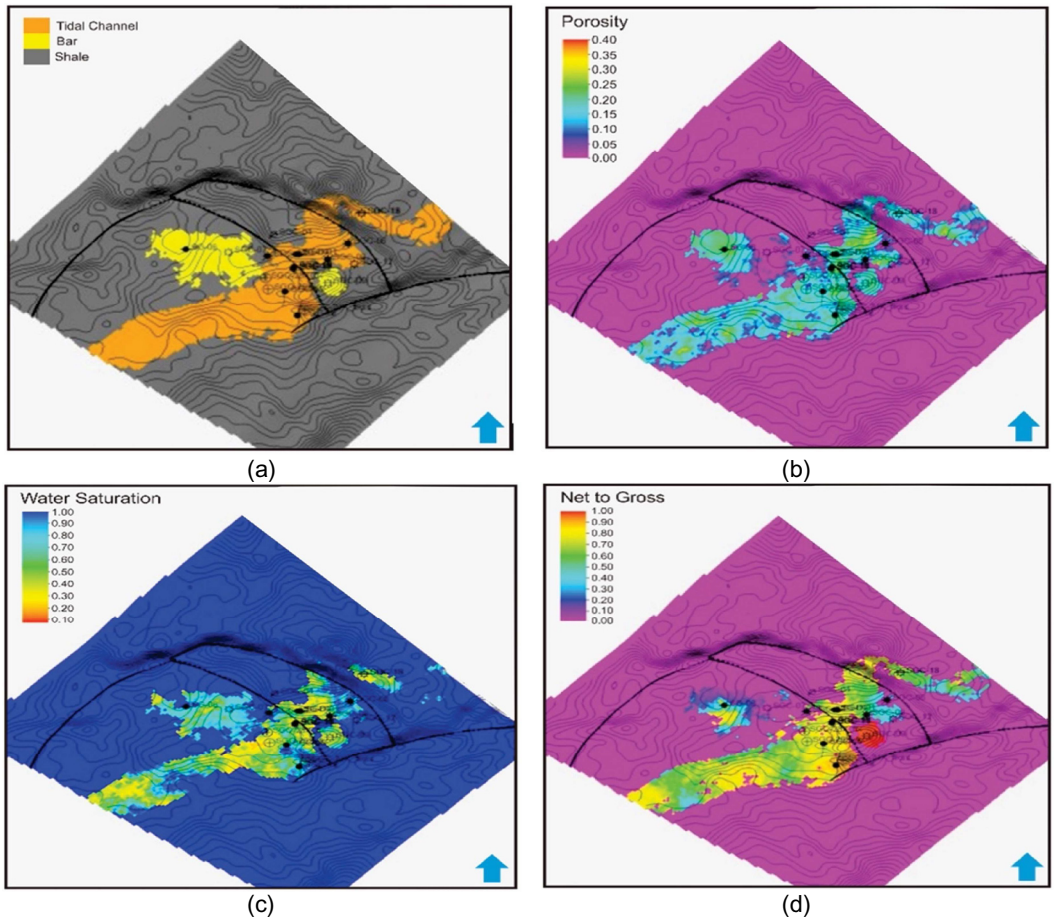

Fig. 8. The modeling of petrophysical properties for the reservoir of layer N, which is illustrated by (a) Facies, (b) porosity, (c) water saturation, and (d) net/gross map.

NE to SW and an ultimate southwestward direction. Depositional environments of the area are also generally characterized by the potential paleocurrent direction within the channel axis from NE to SW, with respective agreement from larger scale porosity and net/gross models.

CONCLUSIONS

Herein, a successful reservoir model of an oil field in Jambi Sub-basin, Sumatra, Indonesia is presented. The model was formulated by integrating geological and geophysical approaches, with particular attention to lateral distributions of petrophysical properties of the targeted layer, such as porosity, water saturation, and net/gross. The geometrical framework of the study area comprises a two-fault system with NE-SW trending, and its tips are terminated by normal fault occurrences inside the system. These features are associated with the latest tectonic phase, which was reactivated by the Pliocene-Pleistocene orogenesis that formed massive folds and a fault in a NW direction. The reservoir model is strongly influenced by facies modeling, which illustrates meandering to a braided type tidal channel that was likely developed under marine fan conditions and, in turn, propagated a tidal sand deposit. The geological aspect of the reservoir model is well represented by the gross depositional environment, which is primarily considered a transition zone to shallow marine deposits. These were specifically located in a submarine fan channel with a plain to the moderately steep angle of its sedimentation base.

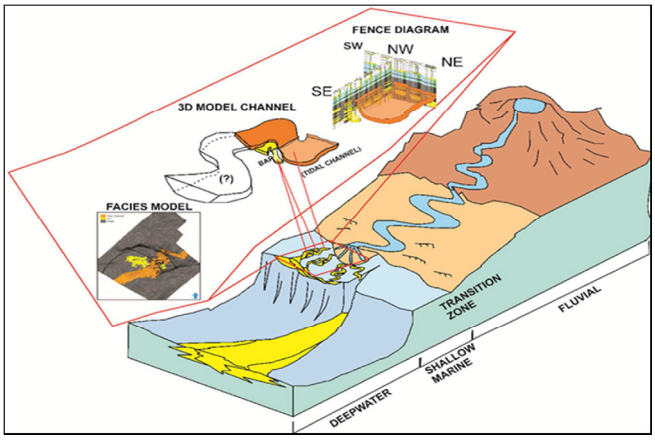

Fig. 9. The fence diagram analysis of the orientation and geometry of the channel, which meanders from NE to SW and ultimately continues in a SW direction.

Acknowledgments: The author would like to thank Applied Research Grant 2019 from Ministry of Research, Technology and Higher Education, Republic of Indonesia for supporting this fund's research and Schlumberger for facilitating the Petrel software for reservoir modeling. Moreover, the author hope that this paper might be useful for scientific developments, especially in reservoir geosciences.

References

Allen, J.L., Johnson, C.L. (2011) Architecture and formation of transgressive-regressive cycles in marginal marine strata of the John Henry Member, Straight Cliffs Formation, Upper Cretaceous of Southern Utah, USA.

Sedimentology, v.58(6), pp.1486-1513. DOI: 10.1111/j.1365-3091.2010.01223.x

Al-Eidan, A.J., Wethington, W.B., Davies, R.B. (2001) Upper Burgan reservoir description, northern Kuwait: impact on reservoir development. GeoArabia, v.6(2), pp.179-208.

Archie, G.E. (1950) Introduction to petrophysics of reservoir rocks. AAPG bull, 34(5): 943-961.

Argakoesoemah, R.M.I., Kamal, A. (2004) Ancient Talang Akar deepwater sediments in South Sumatra Basin: a new exploration play. *In* Proceedings Indonesian Petroleum Association-American Associaion of Petroleum Geologists Deepwater and Frontier Exploration In Asia & Australasia Symposium, Jakarta, Indonesia, pp. 251-267.

Ariani, S., Sihombing, A.Y., Gunawan, I.M., Setiawan, A., Adam, P., Tarmusi, A. (2010) Facies and Sandstone Distribution Pattern of "X" Sandstone Reservoir in Air Benakat Formation, Sungai Gelam Field, Jambi Subbasin. *In* Proceedings Indonesian Petroleum Association 34th Annual Convention, Jakarta, pp. IPA10-G-167

Bishop, M.G. (2001) South Sumatra Basin Province, Indonesia: The Lahat/Talang Akar-Cenozoic Total Petroleum System. USGS 99-50-S. USA.

Bornard, R., Allo, F., Coléou, T., Freudenreich, Y., Caldwell, D.H., Hamman, J.G. (2005) Petrophysical Seismic Inversion to Determine More Accurate and Precise Reservoir Properties. *In* Proceedings of 67th EAGE Conference & Exhibition, pp. SPE94144.

Catuneanu, O. (2006) Sequence stratigraphy of clastic systems: concepts, merits, and pitfalls. J Afr Earth Sci 35:1-43. https://doi.org/10.1016/S0899-5362(02)00004-0

Corbel, S., Wellmann, J.F. (2015) Framework for multiple hypothesis testing improves the use of legacy data in structural geological modeling. GeoRes Jour., v.6, pp.202-212. DOI:10.1016/j.grj.2015.04.001

Das, B., Chatterjee, R. (2016). Porosity mapping from inversion of post-stack seismic data. Georesursy, v.18(4), pp.306-313.

Das, B., Chatterjee, R., Singha, D.K., Kumar, R. (2017) Post-stack seismic inversion and attribute analysis in shallow offshore of Krishna-Godavari basin, India. Jour. Geol. Soc. India, v.90(1), pp.32-40.

Das, B., Chatterjee, R. (2018) Well log data analysis for lithology and fluid identification in Krishna-Godavari Basin, India. Arabian Jour. Geosci., v.11(10), pp.231. DOI:10.1007/s12517-018-3587-2

De Coster, G.L. (1974) The Geology of the Central and South Sumatra Basin. *In* Proceedings Indonesian Petroleum Association 3rd Annual Convention, Jakarta, Indonesia, pp.77-110.

dos Anjos CEG, Zucchi H (2001) Geological and geophysical integrated methodology for reservoir characterization. In SPE Latin American and Caribbean Petroleum Engineering Conference. Soc. Petrol. Enggs., pp.SPE-69461-MS.

Elsayed, S.A., Baker, R., Churcher, P.L., Edmunds, A.C. (1993) Multidisciplinary Reservoir Characterization and simulation study of the Weyburn unit. Jour. Petrol. Tech., v.45(10), pp.930-973.

Harding, T.P., Vierbuchen, R.C., Christie-Blick, N. (1985) Structural styles, plate-tectonic settings, and hydrocarbon traps of divergent (transtensional) wrench faults. *In* Proceedings The Society of Economic Paleontologist and Mineralogists, pp.51-77.

Haris, A., Almunawwar, H.A., Riyanto, A., Bachtiar, A. (2017) Shale Hydrocarbon Potential of Brown Shale, Central Sumatera Basin Based on Seismic and Well Data Analysis. In IOP Conference Series: Earth and Environmental Science (Vol. 62, No. 1, p. 012018). IOP Publishing. DOI: 10.1088/1755-1315/62/1/012018

Haris, A., Novriyani, M., Suparno, S., Hidayat, R., Riyanto, A. (2017) Integrated seismic stochastic inversion and multi-attributes to delineate reservoir distribution: Case study MZ fields, Central Sumatra Basin. In AIP Conference Proceedings (Vol. 1862, No. 1, p. 030180). AIP Publishing. DOI: 10.1063/1.4991284

Hoyanagi, K., Ikedzu, D., Shimizu, Y., Omura, A. (2000) Reconstruction of the delta and estuary systems and sequence stratigraphy of the Plio-Pleistocene strata in the Higashikubiki Hills, Niigata Prefecture, central Japan. Chikyu kagaku, v.54, pp.393-404.

Ito, T., Nakajima, T., Xue, Z. (2017) Geological reservoir characterization and modelling of a CO_2 storage aquifer: A case study of the Nagaoka site, Japan. Energy Procedia 114: 2792-2798. DOI: 10.1016/j.egypro.2017.03.1396

Kasim, S.A., Armstrong, J. (2015) Oil-oil correlation of the South Sumatra Basin reservoirs. Jour. Petroleum Gas Engg., v.6(5), pp.54-61. DOI: 10.5897/JPGE 2013.0162

Kumar, R., Das, B., Chatterjee, R., Sain, K. (2016) A methodology of porosity estimation from inversion of post-stack seismic data. Jour. Natural Gas Sci. Engg., v.28, pp.356-364. DOI:10.1016/j.jngse.2015.12.028

Lutz, R., Gaedicke, C., Berglar, K., Schloemer, S., Franke, D., Djajadihardja, Y.S. (2011) Petroleum systems of the Simeulue fore-arc basin, offshore Sumatra, Indonesia. AAPG Bull., v.95(9), pp.1589-1616.

Maulana, H.A., Haris, A. (2018, May) Reservoir and Source Rock Identification Based on Geologycal, Geophysics and Petrophysics Analysis Study Case: South Sumatra Basin. In Journal of Physics: Conference Series (Vol. 1025, No. 1, p. 012127). IOP Publishing. DOI: 10.1088/1742-6596/1025/1/012127

McClay, K., Bonora, M. (2001) Analog models of restraining stepovers in strike-slip fault systems. AAPG Bull., v.85(2), pp.233-260.

Melati, R.A., Apriadi, D. (2018) An Integrated Sequence Stratigraphic Approach and Depositional Facies Analysis of the Talang Akar Formation in the Jambi Merang Area, Jambi Sub-Basin. *In* Proceedings Indonesian Petroleum Association 42nd Annual Convention, Jakarta, Indonesia, pp. IPA18-129-G.

Mitchum, Jr. R.M., Vail, P.R., Thompson, III S. (1977) Seismic stratigraphy and global changes of sea level: Part 2. The depositional sequence as a basic unit for stratigraphic analysis: Section 2. Application of seismic reflection configuration to stratigraphic interpretation, pp. 53-62.

Mode, A.W., Anyiam, O.A., John, S.I. (2017) Depositional environment and reservoir quality assessment of the "Bruks Field," Niger Delta. Jour. Petroleum Exploration and Production Tech., v.7(4), pp.991-1002.

Moradi, S., Moeini, M., al-Askari, M.K.G., Mahvelati, E.H. (2016) Determination of Shale Volume and Distribution Patterns and Effective Porosity from Well Log Data Based On Cross-Plot Approach for A Shaly Carbonate Gas Reservoir. In IOP Conference Series: Earth and Environmental Science (Vol. 44, No. 4, p. 042002). IOP Publishing. DOI: 10.1088/1755-1315/44/4/042002

Poupon, A., Leveaux, J. (1971) Evaluation of water saturation in shaly formations. In SPWLA 12th Annual Logging Symposium. Society of Petrophysicists and Well-Log Analysts, pp.SPWLA-1971-vXIIn4a1.

Pyrcz, M.J., Deutsch, C.V. (2014) Geostatistical reservoir modeling. Oxford University Press.

Rizaldi, A.R., Fauzi, F. (2015) Application of Lift Technique before Spectral Decomposition to Re-Model Channel Distribution in the Sungai Gelam Field, Jambi. *In* Proceedings Indonesian Petroleum Association 37th Annual Convention, Jakarta, Indonesia, pp. IPA13-G-068.

Rudd, R.A., Tulot, S., Siahaan, D. (2013) Rejuvenating Play Based Exploration Concept in South Sumatra Basin. In Proceedings Indonesian Petroleum Association 39th Annual Convention, Jakarta, Indonesia, pp. IPA15-G-136.

Rui, Z., Cui, K., Wang, X., Chun, J., Li Y., Zhang, Z., Lu, J., Chen, G., Zhou, X., Patil, S. (2018) A Comprehensive Investigation on Performance of Oil and Gas Development in Nigeria: Technical and Non-Technical Analyses. Energy 158:666-680. DOI:10.1016/j.energy.2018.06.027

Sarjono, S. (1989) Hydrocarbon source rock identification in the South Palembang Sub-basin. In Proceedings Indonesian Petroleum Association 18th Annual Convention, Jakarta, Indonesia, v.1, pp.427-467.

Scholle, P.A., Spearing, D. (Eds.). (1982) Sandstone Depositional Environments: AAPG Mem. no.31.

Shedid, S.A., Saad, M.A. (2017) Analysis and field applications of water saturation models in shaly reservoirs. Jour. Petrol. Gas Engg., v.8(10), pp.11-122.

Sprague, A.R., Garfield, T.R., Goulding, F.J., Beaubouef, R.T., Sullivan, M.D., Rossen, C., Campion, K.M., Sickafoose, D.K., Abreu, V, Schellpeper, M.E., Jensen, G.N. (2005) Integrated slope channel depositional models: the key to successful prediction of reservoir presence and quality in offshore West Africa. CIPM, cuarto E-Exitep. P.1e13.

Susanto, R.A. (2009) A Reservoir Engineering Study of Gelam Field to Understand Compartmentalization. In Proceedings Indonesian Petroleum Association 33rd Annual Convention, Jakarta, Indonesia, pp. IPA09-E-160.

van Bemmelen, R.W. (1949) Report on the volcanic activity and volcanological research in Indonesia during the period 1936-1948. Bull. Volcanologique, v.9(1), pp.3-29.

(Received: 29 May 2019; Revised form accepted: 17 October 2019)